Robust Switched Control with Guaranteed Cost of a Furuta Pendulum Prototype using T-S Fuzzy model*

Uiliam N. L. T. Alves
Federal Institute of Paraná - IFPR,
Campus of Jacarezinho
Jacarezinho - PR, Brazil, 86.400-000
uiliam.alves@ifpr.edu.br

Ricardo Breganon
Federal Institute of Paraná - IFPR,
Campus of Jacarezinho
Jacarezinho - PR, Brazil, 86.400-000
ricardo.breganon@ifpr.edu.br

Hugo F. Yamanaka
Dept. of Electrical Engineering
São Paulo State University - UNESP
Ilha Solteira - SP, Brazil, 15.385-000
hugo.yamanaka@unesp.br

Dante J. S. Oncoy
Dept. of Electrical Engineering
São Paulo State University - UNESP
Ilha Solteira - SP, Brazil, 15.385-000
dante.solis-oncoy@unesp.br

Flávio A. Faria
Dept. of Mathematics - School of Engineering
São Paulo State University - UNESP
Ilha Solteira - SP, Brazil, 15.385-000
flavio.faria@unesp.br

Marcelo C. M. Teixeira
Dept. of Electrical Engineering
São Paulo State University - UNESP
Ilha Solteira - SP, Brazil, 15.385-000
marcelo.minhoto@unesp.br

***Abstract*—Takagi-Sugeno (T-S) fuzzy models provide an exact representation for a broad class nonlinear systems within defined operating regions. This work addresses the complexity of such models by representing selected nonlinearities through polytopic vertices and treating the remaining ones as norm-bounded terms. We propose a switched control strategy with guaranteed cost performance, where the controller gains are synthesized based on local models, offering a balanced alternative: it is less conservative than a single state-feedback gain, yet more computationally efficient than Parallel Distributed Compensation (PDC), as it eliminates the need for online membership function calculations in the control signal. Design conditions based on Linear Matrix Inequalities (LMIs) are presented. The method is experimentally validated on a Furuta pendulum prototype, with results confirming reduced conservatism and effective real-time operation under disturbances.**

***Index Terms*—Robust switched control, Guaranteed cost, Uncertain T-S fuzzy model, Furuta pendulum**

I. INTRODUCTION

Takagi-Sugeno (T-S) fuzzy models have become a powerful tool for exactly representing nonlinear dynamic systems. However, a practical limitation is the exponential growth in the number of local models required to describe systems with multiple nonlinearities. This growth increases analytical and computational complexity. It hinders both controller synthesis and practical implementation by requiring the evaluation of a large number of complex membership functions. Nonetheless, norm-bounded uncertainties can be used to reduce the number of local models [1].

A classical structure for T-S fuzzy control is the Parallel Distributed Compensation (PDC) [2]. It combines the gains of all local models and the respective membership functions simultaneously to compute the control signal. To mitigate the inherent complexity of this approach, switched control strategies have been investigated [3, 4]. In this approach, only one controller associated with a local model is activated at a time, according to a switching law. This substantially reduces the computational burden of online control signal computation compared to PDC. Switched control can also lead to less conservative design conditions than a single feedback gain valid for the entire polytope [5], and this advantage is maintained in other control structures. For example, in switched derivative feedback [6] and in switched non-PDC controllers [7]. However, even in switched configurations, the number of models, and thus the gains to be designed a priori, can remain high for complex systems using only a polytopic representation.

Inverted and rotary pendulum systems are classic and widely adopted benchmarks in control theory, ideal for testing and comparing control strategies due to their inherent nonlinearity, instability, and underactuated nature [8, 9]. Among these, the Furuta pendulum [10–12] presents a particularly compelling case study. Its complex, coupled dynamics and the challenging objective of balancing the pendulum in its inverted position make it an excellent platform to validate advanced control methodologies, such as the switched control strategy proposed in this work.

This paper employs an approach that combines a polytopic description of part of the nonlinearities with norm-bounded uncertainties. This combination yields a T-S fuzzy model with fewer vertices. For this system, the switched control law with guaranteed cost proposed in [13] is adapted. This guaranteed cost criterion not only ensures stability but also allows minimizing an upper bound on the output signal energy. The effectiveness of the proposal is demonstrated experimentally by controlling a real Furuta pendulum. The pendulum is subjected to disturbances and uses rods of different masses and lengths, validating the robustness and practicality of the approach.

The contributions of this paper are:

*This study was financed by the "Conselho Nacional de Desenvolvimento Científico e Tecnológico - Brazil (CNPq) - Grant 308581/2022-9", and the "São Paulo Research Foundation (FAPESP) under Grant 2023/05700-2 and Grant 2024/20978-0".

- It presents a mixed-representation T-S fuzzy model for the Furuta pendulum, combining polytopic descriptions of selected nonlinearities with norm-bounded representations of the remaining ones, thereby reducing the number of vertices in the model.
- It derives LMI conditions for synthesizing a switched control law with guaranteed cost for the mixed-representation T-S fuzzy model. This control law does not require online computation of membership functions, eliminating this computational complexity from the implementation and being more efficient than using a single feedback gain.
- It experimentally validates the proposed control on a real prototype, demonstrating the robustness of the switched control under disturbances and parameter changes (two different rods).

Notation: The explicit dependence on time (t) is omitted from variables unless necessary for clarity. For symmetric block matrices, the symbol $\star$ denotes the symmetric blocks. The block-diagonal matrix formed by the matrices $M_1, \cdots, M_r$ is indicated by $\mathrm{diag}\{M_1, \cdots, M_r\}$. $M > 0$ ($M < 0$, $M \geq 0$, and $M \leq 0$) means that the matrix M is symmetric and positive definite (negative definite, positive semi-definite, and negative semi-definite, respectively). $0_{n\times m}$ and I_n represent the null matrix and identity matrix of order $n \times m$ and $n \times n$, respectively. $\mathbb{K}_r = \{1, 2, \cdots, r\}$, $r \in \mathbb{N}$. $j = \arg\min^*_{k\in\mathbb{K}_r} \{h_k\}$ represents the lowest index $j \in \mathbb{K}_r$ such that $h_j = \min_{k\in\mathbb{K}_r} \{h_k\}$. A generic matrix $M_\alpha \in \Re^{n\times m}$ is defined as a convex combination of known matrices M_i such that

$$M_\alpha = \sum_{i=1}^{r} \alpha_i M_i,\ M_i \in \Re^{n\times m},\ \alpha_i \geq 0,\ \sum_{i=1}^{r} \alpha_i = 1,\ i \in \mathbb{K}_r.$$

Data and Code Availability: The designed controller, code, and data obtained in this work are available in [14].

II. Furuta Pendulum Prototype

Fig. 1 presents the Furuta pendulum prototype used in the experiments. It consists of an updated version of the prototype used in [12]. For the rotational motion of the system, a 12 V brushless DC motor manufactured by Maxon® 1 is employed. The angular position of the motor shaft is measured by a HEDS-5540 incremental encoder with a resolution of 500 PPR (pulses per revolution), directly coupled to the shaft. The prototype's arm 2 is made of aluminum and is fixed to the motor shaft at one end. At the other end of the arm, there is an LPD3806-600BM-G5-24C 600 PPR incremental encoder 3, used to measure the angular position of the rod (pendulum). The electrical power for the motor and encoders is provided by a DC power supply 4. The data acquisition system, which reads sensor signals and sends commands to the actuator, comprises a LAUNCHXL-F28379D board from Texas Instruments® 5, connected to the computer via a USB interface. The control strategy is implemented in MATLAB/Simulink® software, running on a 12th Gen Intel® Core™ i5-12500 (3 GHz) computer with 8 GB of RAM 6.

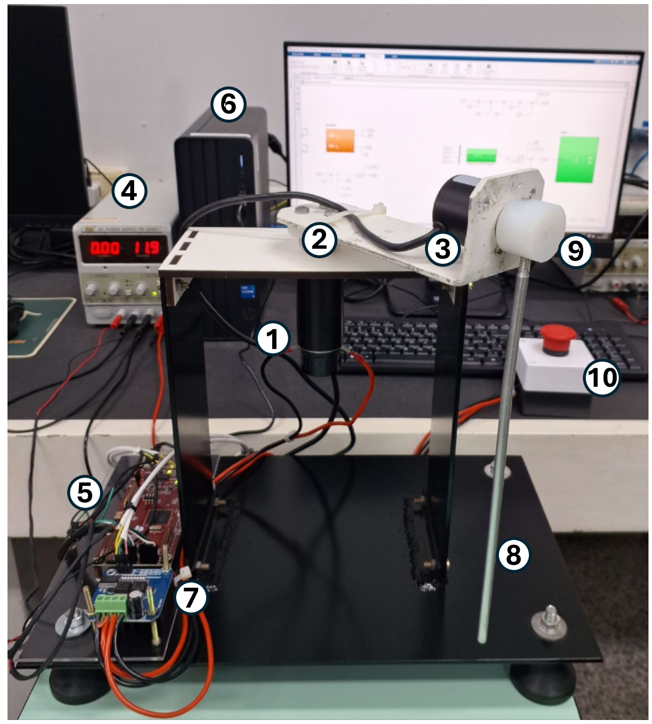

Fig. 1. Furuta Pendulum prototype in the Industrial Automation and Control Laboratory - IFPR/Jacarezinho.

The calculated control signal is sent to a 43A-BTS 7960 - IBT-2 H-bridge 7, which applies the corresponding voltage to the DC motor to control its direction and speed. The prototype operates at a sampling rate of 1 ms. The control objective for this prototype is to stabilize the pendulum rod 8 in the inverted position. This rod is connected to the encoder through a nylon coupling 9. To ensure equipment integrity and safety during experimental tests, the prototype features an emergency stop button 10.

III. Furuta Pendulum T-S Fuzzy Model

The complete model of the Furuta pendulum prototype comprises both the mechanical equations of motion and the actuator torque dynamics (electric motor). Let θ_1 be the arm angle and θ_2 the rod angle, with τ_1, τ_2, and g representing the torques applied to the arm and rod, and the gravitational acceleration, respectively. The equations of motion are [11]:

$$\begin{bmatrix} \ddot{\theta}_1 \\ \ddot{\theta}_2 \end{bmatrix} = \frac{1}{\Delta} \begin{bmatrix} \mathcal{F}_1 \\ \mathcal{F}_2 \end{bmatrix} \begin{bmatrix} \dot{\theta}_1 \\ \dot{\theta}_2 \\ \dot{\theta}_1\dot{\theta}_2 \\ \dot{\theta}_1^2 \\ \dot{\theta}_2^2 \end{bmatrix} + \frac{1}{\Delta} \begin{bmatrix} \mathcal{G}_1 \\ \mathcal{G}_2 \end{bmatrix} \begin{bmatrix} \tau_1 \\ \tau_2 \\ g \end{bmatrix}, \tag{1}$$

$$\Delta = \hat{J}_2\big(\hat{J}_0 + \hat{J}_2 \sin^2(\theta_2)\big) - (m_2 L_1 l_2)^2 \cos^2(\theta_2),$$

$$\mathcal{F}_1^T = \begin{bmatrix} \mathcal{F}_{11} \\ \mathcal{F}_{12} \\ \mathcal{F}_{13} \\ \mathcal{F}_{14} \\ \mathcal{F}_{15} \end{bmatrix} = \begin{bmatrix} -\hat{J}_2 b_1 \\ m_2 L_1 l_2 b_2 \cos(\theta_2) \\ -\hat{J}_2^2 \sin(2\theta_2) \\ -\frac{1}{2}\hat{J}_2 m_2 L_1 l_2 \cos(\theta_2)\sin(2\theta_2) \\ \hat{J}_2 m_2 L_1 l_2 \sin(\theta_2) \end{bmatrix},$$

$$\mathcal{G}_1^T=\begin{bmatrix}\mathcal{G}_{11}\\ \mathcal{G}_{12}\\ \mathcal{G}_{13}\end{bmatrix}=\begin{bmatrix}\hat{J}_2\\ -m_2L_1l_2\cos(\theta_2)\\ m_2^2l_2^2L_1\cos(\theta_2)\sin(\theta_2)\end{bmatrix},$$

$$\mathcal{F}_2^T=\begin{bmatrix}\mathcal{F}_{21}\\ \mathcal{F}_{22}\\ \mathcal{F}_{23}\\ \mathcal{F}_{24}\\ \mathcal{F}_{25}\end{bmatrix}=\begin{bmatrix}m_2L_1l_2b_1\cos(\theta_2)\\ -b_2(\hat{J}_0+\hat{J}_2\sin^2(\theta_2))\\ m_2L_1l_2\hat{J}_2\cos(\theta_2)\sin(2\theta_2)\\ 0.5\hat{J}_2(\hat{J}_0+\hat{J}_2\sin^2(\theta_2))\sin(2\theta_2)\\ -m_2^2L_1^2l_2^2\cos(\theta_2)\sin(\theta_2)\end{bmatrix},$$

$$\mathcal{G}_2^T=\begin{bmatrix}\mathcal{G}_{21}\\ \mathcal{G}_{22}\\ \mathcal{G}_{23}\end{bmatrix}=\begin{bmatrix}-m_2L_1l_2\cos(\theta_2)\\ (\hat{J}_0+\hat{J}_2\sin^2(\theta_2))\\ -m_2l_2(\hat{J}_0+\hat{J}_2\sin^2(\theta_2))\sin(\theta_2)\end{bmatrix}.$$

The variables in (1) are described in [11, 12], and their values can be found in [12, 14]. Equation (1) can be rewritten as

$$\begin{bmatrix}\ddot{\theta}_1\\ \ddot{\theta}_2\end{bmatrix}=\begin{bmatrix}\tilde{A}_{33} & \tilde{A}_{34}\\ \tilde{A}_{43} & \tilde{A}_{44}\end{bmatrix}\begin{bmatrix}\dot{\theta}_1\\ \dot{\theta}_2\end{bmatrix}+\begin{bmatrix}\tilde{B}_{31} & \tilde{B}_{32}\\ \tilde{B}_{41} & \tilde{B}_{42}\end{bmatrix}\begin{bmatrix}\tau_1\\ \tau_2\end{bmatrix}+\begin{bmatrix}\tilde{A}_{32}\\ \tilde{A}_{42}\end{bmatrix}, \quad (2)$$

$$\begin{aligned}
&\tilde{A}_{32}=\tfrac{1}{\Delta}g\,\mathcal{G}_{13}, \quad \tilde{A}_{33}=\tfrac{1}{\Delta}\left(\mathcal{F}_{11}+\mathcal{F}_{13}\dot{\theta}_2+\mathcal{F}_{14}\dot{\theta}_1\right),\\
&\tilde{A}_{34}=\tfrac{1}{\Delta}\left(\mathcal{F}_{12}+\mathcal{F}_{15}\dot{\theta}_2\right), \quad \tilde{A}_{42}=\tfrac{1}{\Delta}g\,\mathcal{G}_{23},\\
&\tilde{A}_{43}=\tfrac{1}{\Delta}\left(\mathcal{F}_{21}+\mathcal{F}_{23}\dot{\theta}_2+\mathcal{F}_{24}\dot{\theta}_1\right), \quad \tilde{B}_{31}=\tfrac{1}{\Delta}\mathcal{G}_{11},\\
&\tilde{A}_{44}=\tfrac{1}{\Delta}\left(\mathcal{F}_{22}+\mathcal{F}_{25}\dot{\theta}_2\right), \quad \tilde{B}_{32}=\tfrac{1}{\Delta}\mathcal{G}_{21},\\
&\tilde{B}_{41}=\tfrac{1}{\Delta}\mathcal{G}_{12}, \quad \tilde{B}_{42}=\tfrac{1}{\Delta}\mathcal{G}_{22}.
\end{aligned}$$

For a motor with negligible inductance, the motor dynamics reduce to $R_mi+K_m\dot{\theta}_1=V$, or

$$i=-\tfrac{K_m}{R_m}\dot{\theta}_1+\tfrac{1}{R_m}V, \quad (3)$$

where V is the voltage applied to the motor, and R_m and K_m are parameters described in [11, 12]. The motor's produced torque is $\tau_1=K_mi$ [11]; thus, from (3), we obtain

$$\tau_1=-\tfrac{K_m^2}{R_m}\dot{\theta}_1+\tfrac{K_m}{R_m}V. \quad (4)$$

Therefore, the complete Furuta pendulum dynamics are derived from (2) and (4) as

$$\begin{bmatrix}\ddot{\theta}_1\\ \ddot{\theta}_2\end{bmatrix}=\begin{bmatrix}\left(\tilde{A}_{33}-\tilde{B}_{31}\frac{K_m^2}{R_m}\right) & \tilde{A}_{34}\\ \left(\tilde{A}_{43}-\tilde{B}_{41}\frac{K_m^2}{R_m}\right) & \tilde{A}_{44}\end{bmatrix}\begin{bmatrix}\dot{\theta}_1\\ \dot{\theta}_2\end{bmatrix}+\begin{bmatrix}\tilde{B}_{31}\frac{K_m}{R_m}\\ \tilde{B}_{41}\frac{K_m}{R_m}\end{bmatrix}V+\begin{bmatrix}\tilde{B}_{32}\\ \tilde{B}_{42}\end{bmatrix}\tau_2+\begin{bmatrix}\tilde{A}_{32}\\ \tilde{A}_{42}\end{bmatrix}. \quad (5)$$

Now, consider a system described by

$$\dot{x}(t)=f(x(t),u(t)) \quad (6)$$

and an equilibrium point (x_e,u_e) such that $f(x_e,u_e)=0$. We aim to represent system (6) around (x_e,u_e). Let $\Delta x(t)=x(t)-x_e$ and $\Delta u(t)=u(t)-u_e$. Note that $\Delta\dot{x}(t)=x(t)$ and, from (6):

$$\Delta\dot{x}(t)=f(x(t),u(t))=f(\Delta x(t)+x_e,\Delta u(t)+u_e). \quad (7)$$

For the Furuta pendulum, define the state vector as $x(t)=\begin{bmatrix}x_1(t) & x_2(t) & x_3(t) & x_4(t)\end{bmatrix}^T=\begin{bmatrix}\theta_1(t) & \theta_2(t) & \dot{\theta}_1(t) & \dot{\theta}_2(t)\end{bmatrix}^T$. The equilibrium point of interest is the inverted vertical position, with θ_{1e} and θ_{2e} in rad and $\dot{\theta}_{1e}$ and $\dot{\theta}_{2e}$ in rad/s:

$$x_e=\begin{bmatrix}\theta_{1e} & \theta_{2e} & \dot{\theta}_{1e} & \dot{\theta}_{2e}\end{bmatrix}^T=\begin{bmatrix}0 & \pi & 0 & 0\end{bmatrix}^T. \quad (8)$$

Hence,

$$\Delta x(t)=x(t)-x_e=\begin{bmatrix}x_1(t) & x_2(t)-\pi & \dot{x}_1(t) & \dot{x}_2(t)\end{bmatrix}^T. \quad (9)$$

Let the control signal be $u(t)=V$, the disturbance $d(t)=\tau_2$, the state vector (9), and $\hat{x}(t)=\Delta x(t)+x_e$. The Furuta pendulum dynamics around the equilibrium point (8) can be described, using (5), (6), and (7), by

$$\begin{aligned}
&\Delta\dot{x}(t)=A(\hat{x})\Delta x(t)+B(\hat{x})u(t)+F(\hat{x})d(t),\\
&[A(\hat{x})|B(\hat{x})|F(\hat{x})]=\left[\begin{array}{cccc|c|c}0&0&1&0&0&0\\0&0&0&1&0&0\\0&A_{32}&A_{33}&A_{34}&B_{31}&\tilde{B}_{32}\\0&A_{42}&A_{43}&A_{44}&B_{41}&\tilde{B}_{42}\end{array}\right]. \quad (10)
\end{aligned}$$

$$\begin{aligned}
&A_{32}=\tfrac{\tilde{A}_{32}}{\Delta x_2}, \quad A_{33}=\left(\tilde{A}_{33}-\tilde{B}_{31}\tfrac{K_m^2}{R_m}\right), \quad A_{34}=\tilde{A}_{34},\\
&A_{42}=\tfrac{\tilde{A}_{42}}{\Delta x_2}, \quad A_{43}=\left(\tilde{A}_{43}-\tilde{B}_{41}\tfrac{K_m^2}{R_m}\right), \quad A_{44}=\tilde{A}_{44},\\
&B_{31}=\tilde{B}_{31}\tfrac{K_m}{R_m}, \quad B_{41}=\tilde{B}_{41}\tfrac{K_m}{R_m}.
\end{aligned}$$

For the fuzzy model, in addition to state variable bounds, we consider the pendulum rod mass and length as uncertain parameters (variables m_2 and L_2). Thus, the following domain is used for the fuzzy model, with m_2 in kg and L_2 in m:

$$\begin{aligned}
&\mathcal{S}=\{z(t)=[\Delta x(t)^T \;\; m_2 \;\; L_2]^T\in\Re^6:\\
&-0.2618\le\Delta x_2(t)\le 0.2618, \;\; -0.5\le\Delta x_3(t),\Delta x_4(t)\le 0.5,\\
&0.01712\le m_2\le 0.02411, \;\; 0.2\le L_2\le 0.2841\}. \quad (11)
\end{aligned}$$

For domain $\mathcal{S}$ in (11), the maximum and minimum values of the nonlinearities in model (10) for matrices $A(\hat{x})$ and $B(\hat{x})$ are presented in Table I, where $\mathcal{M}_{ij}(\mathcal{E}_{ij})=\left(\max_{z(t)\in\mathcal{S}}\{\mathcal{E}_{ij}\}-\min_{z(t)\in\mathcal{S}}\{\mathcal{E}_{ij}\}\right)/2$, $\mathcal{R}_{ij}(\mathcal{E}_{ij})=\max_{z(t)\in\mathcal{S}}\{\mathcal{E}_{ij}\}-\mathcal{M}_{ij}(\mathcal{E}_{ij})$, which corresponds to the maximum deviation from the midpoint $\mathcal{M}_{ij}(\mathcal{E}_{ij})$, and $\delta_{ij}(\mathcal{E}_{ij})=\sqrt{\mathcal{R}_{ij}(\mathcal{E}_{ij})}$.

Note that each nonlinearity can be expressed in the form $\mathcal{E}_{ij}=\mathcal{M}_{ij}(\mathcal{E}_{ij})+\delta_{ij}(\mathcal{E}_{ij})\,\vartheta(z)\,\delta_{ij}(\mathcal{E}_{ij})$, where $\vartheta(z)$ is an uncertain scalar function satisfying $-1\le\vartheta(z)\le 1$, z defined in (11). This representation allows the term $\mathcal{E}_{ij}$ to be treated as its midvalue with norm-bounded uncertainty.

Using the values in Table I, the Furuta pendulum dynamics around the inverted vertical position can be represented by the model

$$\begin{aligned}
&\dot{x}(t)=A_\alpha x(t)+B_\alpha u(t)+E_1\,\Delta_1\,F_1x(t)+E_2\,\Delta_2\,F_2\,u(t),\\
&y(t)=C_\alpha x(t), \quad (12)
\end{aligned}$$

where $\Delta_1^T\Delta_1\le I_{n_A}$ and $\Delta_2^T\Delta_2\le I_{n_B}$, n_r is the number of vertices, and n_A and n_B are the numbers of nonlinearities treated as norm-bounded uncertainties in matrices A and B, respectively.

TABLE I
UNCERTAIN NONLINEARITIES CHARACTERISTICS OF THE FURUTA PENDULUM PROTOTYPE DYNAMICS (10) IN (11).

Entry $\mathcal{E}_{ij}$	min.	max.	$\mathcal{M}_{ij}(\mathcal{E}_{ij})$	$\mathcal{R}_{ij}(\mathcal{E}_{ij})$	$\delta_{ij}(\mathcal{E}_{ij})$
A_{42}	54.9500	81.6960	68.3230	13.3730	3.6569
B_{41}	5.0606	7.6148	6.3377	1.2771	1.1301
A_{32}	4.5943	6.8011	5.6977	1.1034	1.0504
A_{44}	-1.4477	-0.5080	-0.9779	0.4699	0.6854
A_{43}	-0.5407	-0.0975	-0.3191	0.2216	0.4708
B_{31}	5.8553	6.0282	5.9418	0.0865	0.2940
A_{33}	-0.3610	-0.2574	-0.3092	0.0518	0.2276
A_{34}	-0.0957	-0.0422	-0.0690	0.0268	0.1636

Remark 1. *Considering uncertain parameters in the domain* (11) *yields uncertain membership functions that cannot be used directly in the computation of the control signal. The switched control approach from [3, 4] provides a way to handle these uncertain membership functions. Nevertheless, the fuzzy modeling framework remains essential for defining the local models used in the switched controller design.*

For model (12), consider $s = 4$ polytopic uncertainties given by A_{42}, B_{41}, A_{32}, and A_{44}, resulting in $n_r = 2^s = 16$ vertices. Additionally, let $n_A = 3$ and $n_B = 1$ be the nonlinear terms represented by norm-bounded uncertainties in matrices A and B, respectively, given by A_{33}, A_{34}, A_{43}, and B_{31}. Thus, using the data in Table I, the matrices in (12) are

$$E_1 = \begin{bmatrix} 0 & 0 & 0 \\ 0 & 0 & 0 \\ 0.2276 & 0.1635 & 0 \\ 0 & 0 & 0.4708 \end{bmatrix},\ E_2 = \begin{bmatrix} 0 \\ 0 \\ 0.2940 \\ 0 \end{bmatrix},$$

$$F_1 = \begin{bmatrix} 0 & 0 & 0.2276 & 0 \\ 0 & 0 & 0 & 0.1635 \\ 0 & 0 & 0.4708 & 0 \end{bmatrix},\ F_2 = 0.2940,$$

$$A_i = \begin{bmatrix} 0 & 0 & 1 & 0 \\ 0 & 0 & 0 & 1 \\ 0 & A_{32} & -0.3092 & -0.0689 \\ 0 & A_{42} & -0.3191 & A_{44} \end{bmatrix}, B_i = \begin{bmatrix} 0 \\ 0 \\ 5.9418 \\ B_{41} \end{bmatrix},$$

$$C_i = C = \begin{bmatrix} 1 & 0 & 0 & 0 \\ 0 & 1 & 0 & 0 \end{bmatrix}. \quad (13)$$

The matrices A_i and B_i correspond to the vertices of a polytopic set are obtained by assigning the lower or upper bound to each uncertain entry A_{32}, A_{42}, A_{44} and B_{41} (Table I). All the matrices are listed in the data set [14].

IV. SWITCHED FUZZY CONTROL OF T-S SYSTEMS WITH NORM-BOUNDED UNCERTAINTY AND GUARANTEED COST

Consider an uncertain nonlinear system exactly represented in a domain $\mathcal{S}$ by the T-S fuzzy model (12), where $\Delta_1^T\Delta_1 \leq I_{n_A}$ and $\Delta_2^T\Delta_2 \leq I_{n_B}$. The model has n_r vertices, with known matrices $A_i \in \Re^{n_x\times n_x}$, $B_i \in \Re^{n_x\times n_u}$, $E_1 \in \Re^{n_x\times n_A}$, $F_1 \in \Re^{n_A\times n_x}$, $E_2 \in \Re^{n_x\times n_B}$, $F_2 \in \Re^{n_B\times n_x}$, and $C_i \in \Re^{n_y\times n_x}$.

The following guaranteed cost based on the output signal energy is considered [13]:

$$J = \int_0^\infty y(t)^T S y(t)\ dt = \int_0^\infty x(t)^T C_\alpha^T S C_\alpha x(t)\ dt, \quad (14)$$

where $S = S^T > 0 \in \Re^{n_y\times n_y}$. The initial condition is described by

$$x(0) = \sum_{m=1}^{n_{x_0}} \lambda_m \mathrm{x}_m, \sum_{m=1}^{n_{x_0}} \lambda_m = 1, \lambda_m \geq 0, m \in \mathbb{K}_{n_{x_0}}, \quad (15)$$

where $\mathrm{x}_m \in \Re^{n_x}$, $m \in \mathbb{K}_{n_{x_0}}$, are known vectors. n_{x_0} is the number of vertices from the initial condition polytope.

Consider a state feedback controller with a single gain given by

$$u(t) = Kx(t), \quad (16)$$

with $K \in \Re^{n_u\times n_x}$, and the switched control law [3, 4]

$$u(t) = K_\sigma x(t), \quad \sigma = \arg \min_{j\in\mathbb{K}_{n_r}}{}^* \{x(t)^T \bar{Q}_j x(t)\}, \quad (17)$$

where $K_j \in \Re^{n_u\times n_x}$ and $\bar{Q}_j \in \Re^{n_x\times n_x}$, $j \in \mathbb{K}_{n_r}$.

A. Controller Desing

Theorem 1. *Consider the fuzzy model* (12) *and the control law* (16)*. Given $\beta \geq 0$, vectors $\mathrm{x}_m \in \Re^{n_x}$, and a matrix $S = S^T > 0 \in \Re^{n_y\times n_y}$, if there exist matrices $X = X^T > 0 \in \Re^{n_x\times n_x}$, $M \in \Re^{n_u\times n_x}$ and scalars $\varepsilon_1 > 0$, $\varepsilon_2 > 0$, and $\delta > 0$ such that*

$$\begin{bmatrix} \mathcal{M}_i & \star & \star & \star \\ F_1X & -\varepsilon_1 I_{n_A} & \star & \star \\ F_2M & 0_{n_B\times n_A} & -\varepsilon_2 I_{n_B} & \star \\ C_iX & 0_{n_y\times n_A} & 0_{n_y\times n_B} & -S^{-1} \end{bmatrix} < 0, \quad (18)$$

$$\begin{bmatrix} \delta & \star \\ \delta \mathrm{x}_m & X \end{bmatrix} \geq 0, \quad (19)$$

for all $i \in \mathbb{K}_{n_r}$ and $m \in \mathbb{K}_{n_{x_0}}$, with $\mathcal{M}_i = A_iX + B_iM + XA_i^T + M^TB_i^T + 2\beta X + \varepsilon_1 E_1E_1^T + \varepsilon_2 E_2E_2^T$, then the control law (16) *with $K = MX^{-1}$ guarantees that the origin $x = 0$ of the closed-loop system* (12) *and* (16) *is globally asymptotically stable with decay rate $\geq \beta$. Furthermore, the performance index* (14) *satisfies $J \leq \delta^{-1}$ for any initial condition described by* (15).

Proof. Consider the Lyapunov function candidate $V(x) = x^TPx$ with $P = P^T > 0$. For the closed-loop system (12) and (16)

$$\dot{V}(x) = x^T\big[(A_\alpha + B_\alpha K)^T P + P(A_\alpha + B_\alpha K)\big]x + 2x^TPE_1\Delta_1F_1x + 2x^TPE_2\Delta_2F_2Kx. \quad (20)$$

Using $\Delta_1^T\Delta_1 \leq I_{n_A}$, $\varepsilon_1 > 0$, and the bounding method from [15], we have

$$\begin{aligned} 2x^TPE_1\Delta_1F_1x &\leq \varepsilon_1\, x^TPE_1E_1^TPx \\ &\quad + \varepsilon_1^{-1}\, x^TF_1^T(\Delta_1^T\Delta_1)F_1x \\ &\leq \varepsilon_1\, x^TPE_1E_1^TPx + \varepsilon_1^{-1}\, x^TF_1^TF_1x. \end{aligned} \quad (21)$$

Similarly, for $\Delta_2^T\Delta_2 \leq I_{n_B}$ and $\varepsilon_2 > 0$,

$$\begin{aligned} 2x^TPE_2\Delta_2F_2Kx &\leq \varepsilon_2\, x^TPE_2E_2^TPx \\ &\quad + \varepsilon_2^{-1}\, x^TK^TF_2^TF_2Kx. \end{aligned} \quad (22)$$

Therefore, from (20), (21), and (22),

$$\dot{V}(x) \leq x^T\big[(A_\alpha + B_\alpha K)^T P + P(A_\alpha + B_\alpha K)\big]x$$

$$+\,\varepsilon_1\,x^TPE_1E_1^TPx+\varepsilon_1^{-1}\,x^TF_1^TF_1x$$
$$+\,\varepsilon_2\,x^TPE_2E_2^TPx+\varepsilon_2^{-1}\,x^TK^TF_2^TF_2Kx. \quad (23)$$

Now, pre- and post-multiplying (18) by $\mathrm{diag}\{P, I_{n_A}, I_{n_B}, I_{n_y}\}$, with $P = P^T = X^{-1}$, and setting $K = MX^{-1} = MP$, then multiplying by $\alpha_i \geq 0$, where $\sum_{i=1}^{n_r}\alpha_i = 1$, and summing from $i = 1$ to n_r, yields

$$\begin{bmatrix} P\mathcal{M}_\alpha P & \star & \star & \star \\ F_1 & -\varepsilon_1 I_{n_A} & \star & \star \\ F_2K & 0_{n_B\times n_A} & -\varepsilon_2 I_{n_B} & \star \\ C_\alpha & 0_{n_y\times n_A} & 0_{n_y\times n_B} & -S^{-1}\end{bmatrix} < 0. \quad (24)$$

Applying the Schur complement successively to (24) gives

$$P\mathcal{M}_\alpha P + C_\alpha^T S C_\alpha + \varepsilon_2^{-1}K^TF_2^TF_2K + \varepsilon_1^{-1}F_1^TF_1 < 0. \quad (25)$$

Noting that $P\mathcal{M}_\alpha P = PA_\alpha + PB_\alpha K + A_\alpha^TP + K^TB_\alpha^TP + \varepsilon_1 PE_1E_1^TP + \varepsilon_2 PE_2E_2^TP + 2\beta P$, it follows from (25) and (23) that

$$\dot V(x) + 2\beta V(x) < -x^TC_\alpha^TSC_\alpha x. \quad (26)$$

From (26), since $S > 0$, we have $\dot V(x) + 2\beta V(x) < 0$, which is a sufficient condition for the asymptotic stability of the origin with a decay rate $\geq \beta$ [16]. Furthermore, because $P > 0$, it follows that $\dot V(x) < -x^TC_\alpha^TSC_\alpha x$. Integrating both sides from 0 to ∞ and using (14) yields

$$J < V(0) = x(0)^TPx(0). \quad (27)$$

Pre- and post-multiplying (19) by $\mathrm{diag}\{\delta^{-1}, I_{n_x}\}$, multiplying by $\lambda_k \geq 0$ with $\sum_{k=1}^{n_{x_0}}\lambda_m = 1$, and summing from $m = 1$ to n_{x_0} [13] gives:

$$\begin{bmatrix}\delta^{-1} & \star \\ x(0) & X\end{bmatrix} \geq 0. \quad (28)$$

Applying the Schur complement to (28) and using (27), we obtain

$$\delta^{-1} \geq x(0)^TPx(0) = V(0) > J. \quad (29)$$

□

Theorem 2. *Consider the fuzzy model* (12) *and the switched control law* (17). *Given $\beta \geq 0$, vectors $x_m \in \Re^{n_x}$, and a matrix $S = S^T > 0 \in \Re^{n_y\times n_y}$, if there exist symmetric matrices $X > 0$, R_i and $Q_i \in \Re^{n_x\times n_x}$, matrices $M_j \in \Re^{n_u\times n_x}$, and scalars $\varepsilon_1 > 0$, $\varepsilon_{2j} > 0$ and $\delta > 0$ such that*

$$\begin{bmatrix}\mathcal{N}_{1i} & \star & \star \\ F_1X & -\varepsilon_1 I_{n_A} & \star \\ C_iX & 0_{n_y\times n_A} & -S^{-1}\end{bmatrix} < 0, \quad (30)$$

$$\begin{bmatrix}\mathcal{N}_{2ij} & \star \\ F_2M_j & -\varepsilon_{2j}I_{n_B}\end{bmatrix} < 0, \quad (31)$$

and (19) *hold for all $i, j \in \mathbb{K}_{n_r}$, $m \in \mathbb{K}_{n_{x_0}}$, with $\mathcal{N}_{1i} = A_iX + XA_i^T + \varepsilon_1E_1E_1^T + R_i + Q_i + 2\beta X$, $\mathcal{N}_{2ij} = B_iM_j + M_j^TB_i^T + \varepsilon_{2j}E_2E_2^T - R_i - Q_j$, then the control law* (17) *with $K_j = M_jX^{-1}$ and $\bar Q_j = X^{-1}Q_jX$ guarantees that the origin $x = 0$ of the closed-loop system* (12) *and* (17) *is globally asymptotically stable with decay rate $\geq \beta$. Furthermore, the performance index* (14) *satisfies $J \leq \delta^{-1}$ for any initial condition described by* (15).

Proof. Consider the Lyapunov function candidate $V(x) = x^TPx$ with $P = P^T > 0$. For the closed-loop system (12) and (17),

$$\dot V(x) = x^T\big[(A_\alpha + B_\alpha K_\sigma)^TP + P(A_\alpha + B_\alpha K_\sigma)\big]x$$
$$+\,2x^TPE_1\Delta_1F_1x + 2x^TPE_2\Delta_2F_2K_\sigma x. \quad (32)$$

Using $\Delta_1^T\Delta_1 \leq I_{n_A}$, $\Delta_2^T\Delta_2 \leq I_{n_B}$, $\varepsilon_1 > 0$ and $\varepsilon_{2j} > 0$ with $j = \sigma$, the result from [15] gives inequality (21) and

$$2x^TPE_2\Delta_2F_2K_\sigma x \leq \varepsilon_{2\sigma}\,x^TPE_2E_2^TPx$$
$$+\,\varepsilon_{2\sigma}^{-1}\,x^TK_\sigma^TF_2^TF_2K_\sigma x. \quad (33)$$

Therefore, from (32), (21) and (33),

$$\dot V(x) \leq x^T\big[(A_\alpha + B_\alpha K_\sigma)^TP + P(A_\alpha + B_\alpha K_\sigma)\big]x$$
$$+\,\varepsilon_1\,x^TPE_1E_1^TPx + \varepsilon_1^{-1}\,x^TF_1^TF_1x$$
$$+\,\varepsilon_{2\sigma}\,x^TPE_2E_2^TPx + \varepsilon_{2\sigma}^{-1}\,x^TK_\sigma^TF_2^TF_2K_\sigma x. \quad (34)$$

Now, pre- and post-multiplying (30) by $\mathrm{diag}\{P, I_{n_A}, I_{n_y}\}$, with $P = P^T = X^{-1}$, setting $K_j = M_jX^{-1} = M_jP$, $\bar R_j = X^{-1}R_jX^{-1}$, $\bar Q_j = X^{-1}Q_jX^{-1}$, multiplying by $\alpha_i \geq 0$, $\sum_{i=1}^{n_r}\alpha_i = 1$, summing from $i = 1$ to n_r, and applying the Schur complement recursively yields

$$PA_\alpha + A_\alpha^TP + \varepsilon_1PE_1E_1^TP + \bar R_\alpha + \bar Q_\alpha + \varepsilon_1^{-1}F_1^TF_1$$
$$+\,2\beta P + C_\alpha^TSC_\alpha < 0. \quad (35)$$

Next, pre- and post-multiplying (31) by $\mathrm{diag}\{P, I_{n_B}\}$, multiplying by $\alpha_i \geq 0$, $\sum_{i=1}^{n_r}\alpha_i = 1$, summing from $i = 1$ to n_r, for $j = \sigma$, and applying the Schur complement gives

$$PB_\alpha K_\sigma + K_\sigma^TB_\alpha^TP + \varepsilon_{2\sigma}PE_2E_2^TP - \bar R_\alpha - \bar Q_\sigma$$
$$+\,\varepsilon_{2\sigma}^{-1}K_\sigma^TF_1^TF_1K_\sigma < 0. \quad (36)$$

From the switching law (17), we have

$$x(t)^T\bar Q_\sigma x(t) = \min_{i\in\mathbb{K}_{n_r}}\{x(t)^T\bar Q_i x(t)\}$$
$$\leq \sum_{i=1}^{n_r}\alpha_i x(t)^T\bar Q_i x(t) = x(t)^T\bar Q_\alpha x(t). \quad (37)$$

From (34)-(37), and defining $\mathcal{O}_\alpha = PA_\alpha + A_\alpha^TP + \varepsilon_1PE_1E_1^TP + \varepsilon_1^{-1}F_1^TF_1 + 2\beta P + C_\alpha^TSC_\alpha$,

$$\dot V(x) + 2\beta V(x) + x^TC_\alpha^TSC_\alpha x$$
$$\leq x^T\Big(\mathcal{O}_\alpha + PB_\alpha K_\sigma + K_\sigma^TB_\alpha^TP + \varepsilon_{2\sigma}PE_2E_2^TP$$
$$+\,\varepsilon_{2\sigma}^{-1}K_\sigma^TF_1^TF_1K_\sigma\Big)x \leq x^T\Big(\mathcal{O}_\alpha + \bar Q_\alpha + \bar R_\alpha\Big)x < 0.$$

To complete the proof, we follow the same procedure as in the proof of Theorem 1, from (26) to (29). □

Remark 2. *Since δ^{-1} is an upper bound for the guaranteed cost* (14)*, it is desirable to minimize δ^{-1}. From the LMIs in Theorem 1 or Theorem 2, this can be achieved by maximizing δ.*

Theorem 3 (adapted from [17]). *For given constantes $\mu_M > 0$ and $\mu_X > 0$, if the conditions of Theorem 2 (or Theorem 1) hold along with*

$$\begin{bmatrix} X & \star \\ M_j & \mu_M I_{n_u} \end{bmatrix} > 0, \quad X > \mu_X I_{n_x}, \tag{38}$$

for all $j \in \mathbb{K}_{n_r}$ (or using $M_j = M$ for Theorem 1), then $K_j^T K_j < \frac{\mu_M}{\mu_X} I_{n_x}$, where $K_j = M_j X^{-1}$ ($K_j = K = MX^{-1}$ for Theorem 1).

Proof. The proof can be found in [17]. $\square$

V. Results

This section explores how the switched control law (17) can improve the performance index (14) compared to using a single feedback gain (16) for the Furuta Pendulum with local models (13), which are fully described in [14]. Furthermore, the switched control is implemented on the Furuta pendulum prototype described in Section II.

The LMIs were solved using the software MATLAB®, the modeling language YALMIP [18], and the solver LMILab [19]. We used $S = \left[\begin{smallmatrix} 0.001 & 0 \\ 0 & 0.1 \end{smallmatrix}\right]$, $n_{x_0} = 2$, $\mathrm{x}_1 = \begin{bmatrix} 0.5 & 0 & 0 & 0 \end{bmatrix}^T$, $\mathrm{x}_2 = \begin{bmatrix} 0 & 0.5 & 0 & 0 \end{bmatrix}^T$, and $\mu_X = 0.0055$.

A. Example 1 - Optimization of the Guaranteed Cost

As a first example, we compare Theorem 1 (single gain) and Theorem 2 (switched), each with Theorem 3, under different gain-norm constraints and minimum decay rates. The goal is to find the largest value of δ that minimizes the guaranteed cost upper bound (see Remark 2). We also tested different values of μ_M and β.

Fig. 2 shows the results of this comparison. As can be seen, the switched gain (Theorem 2 and 3) achieved a better (larger) guaranteed cost bound than the single feedback gain (Theorem 1 and 3) in every tested scenario.

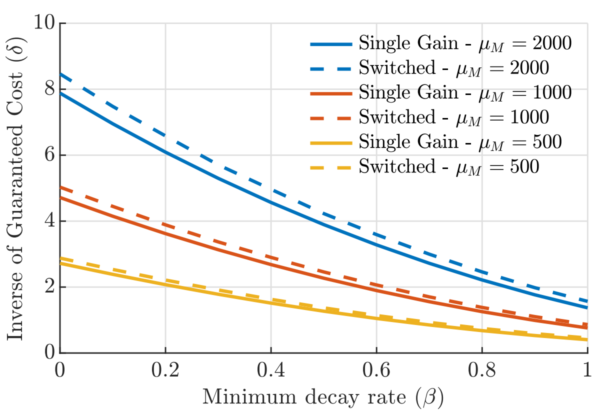

Fig. 2. Maximum values of δ obtained using Theorem 1 (Single Gain) or Theorem 2 (Switched), each with Theorem 3 for fixed μ_X, and different values of μ_M and β.

B. Example 2 - Experimental Results on the Furuta Pendulum Prototype

For the experimental implementation, we set $\mu_M = 2000$ and $\beta = 0.9$, obtaining 16 gains K_j and matrices $\bar{Q}_j$ for the switched control law (17). These matrices are available in [14]. As stated in Remark 1, implementing the control law (17) does not require online computation of membership functions, thus avoiding issues with uncertain membership values.

The implementation results are shown in Fig. 3 for two rod configurations: the short rod ($L_2 = 0.2$ m; $m_2 = 0.01712$ kg) and the long rod ($L_2 = 0.2841$ m; $m_2 = 0.02411$ kg). During the tests, disturbances were intentionally introduced into the control signal to perturb the pendulum's equilibrium. As observed, the proposed controller successfully maintained the pendulum in the inverted position despite the disturbances for both rod configurations. The control signal remained suitable, staying within the ± 12 V limit of the power supply. A video of the experiment is available at https://youtu.be/i5m7Hab6jYk.

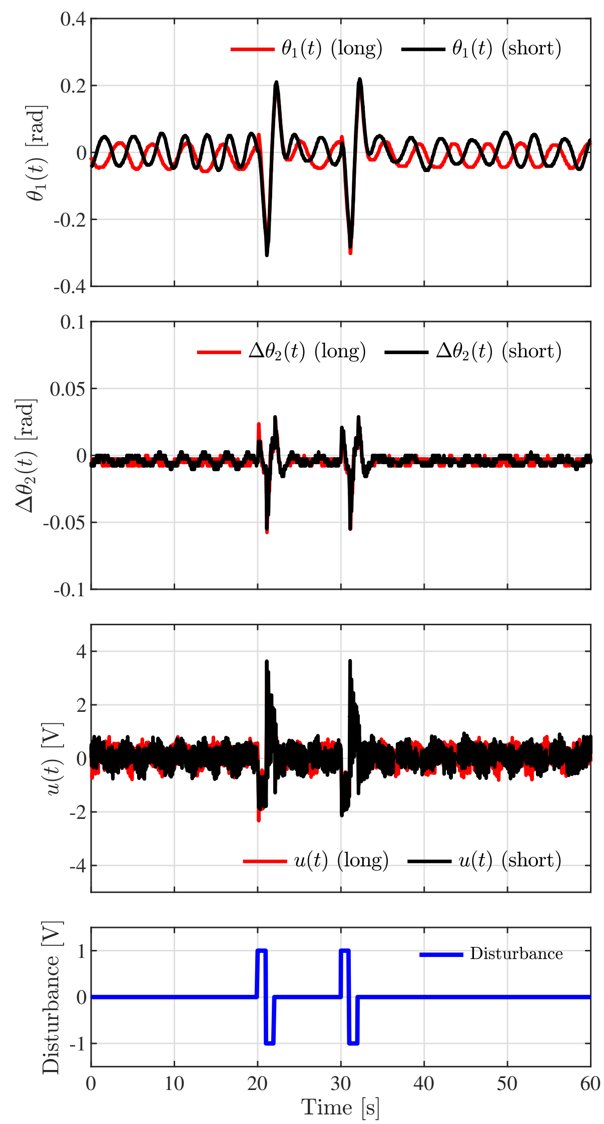

Fig. 3. Experimental results of the switched control (17) implementation on the Furuta pendulum prototype for different rod configurations.

VI. Conclusion

This paper proposes an extension of the switched control strategy previously developed in [3, 4] by incorporating norm-bounded uncertainties into the fuzzy model. The main advantage of this integration was a significant reduction in the number of vertices of the fuzzy model's polytope. This reduction directly leads to a smaller set of LMIs for controller synthesis and a lower computational cost for implementation.

For the system under study, the switched control strategy was shown to be less conservative than employing a single state-feedback gain over the entire polytope, yielding a lower guaranteed performance cost. A key practical benefit is that its implementation avoids online computation of membership functions, thereby simplifying the control algorithm and reducing its computational burden.

The experimental validation of the proposed methodology on the Furuta pendulum prototype, under disturbances and with different rod configurations, successfully demonstrated effectiveness and robustness of the proposed switched control designing for controlling complex, nonlinear, and uncertain systems.

Acknowledgment

The authors would like to thank IFPR and UNESP Campus Ilha Solteira for their support in the development of this work.

References

[1] T. Taniguchi and K. Tanaka, "Model construction, rule reduction, and robust compensation for generalized form of Takagi-Sugeno fuzzy systems," *Fuzzy Systems, IEEE Transactions on*, vol. 9, pp. 525–538, 2001.

[2] H. Wang, K. Tanaka, and M. Griffin, "Parallel distributed compensation of nonlinear systems by Takagi-Sugeno fuzzy model," in *Proceedings of 1995 IEEE International Conference on Fuzzy Systems.*, vol. 2, 1995, pp. 531–538.

[3] W. A. Souza, M. C. M. Teixeira, R. Cardim, and E. Assunção, "On switched regulator design of uncertain nonlinear systems using Takagi-Sugeno fuzzy models," *Fuzzy Systems, IEEE Transactions on*, vol. 22, no. 6, pp. 1720–1727, 2014.

[4] U. N. L. T. Alves, M. C. M. Teixeira, D. R. Oliveira, R. Cardim, E. Assunção, and W. A. Souza, "Smoothing switched control laws for uncertain nonlinear systems subject to actuator saturation," *International Journal of Adaptive Control and Signal Processing*, vol. 30, no. 8-10, pp. 1408–1433, 2016.

[5] W. A. de Souza, M. C. M. Teixeira, M. P. A. Santim, R. Cardim, and E. Assunção, "On switched control design of linear time-invariant systems with polytopic uncertainties," *Mathematical Problems in Engineering*, vol. 2013, no. 1, p. 595029, 2013.

[6] L. D. Wolmuth, U. N. L. T. Alves, A. Krindges, R. Cardim, E. Assunção, and M. C. M. Teixeira, "$\mathcal{H}_\infty$ switched controller design for a class of uncertain linear systems using derivative feedback," *IEEE Access*, vol. 13, pp. 95 034–95 053, 2025.

[7] D. J. S. Oncoy, R. Cardim, F. A. Faria, U. N. L. T. Alves, and M. C. M. Teixeira, "Robust switched non-parallel distributed controller for continuous Takagi-Sugeno fuzzy systems based on generalized Lyapunov function," *International Journal of Fuzzy Systems*, pp. 1–17, 2025.

[8] M. F. Hamza, H. J. Yap, I. A. Choudhury, A. I. Isa, A. Y. Zimit, and T. Kumbasar, "Current development on using rotary inverted pendulum as a benchmark for testing linear and nonlinear control algorithms," *Mechanical Systems and Signal Processing*, vol. 116, pp. 347–369, 2019.

[9] Z. B. Hazem and Z. Bingül, "Comprehensive review of different pendulum structures in engineering applications," *IEEE Access*, vol. 11, pp. 42 862–42 880, 2023.

[10] K. Furuta, M. Yamakita, and S. Kobayashi, "Swing-up control of inverted pendulum using pseudo-state feedback," *Proceedings of the Institution of Mechanical Engineers, Part I: Journal of Systems and Control Engineering*, vol. 206, no. 4, pp. 263–269, 1992.

[11] B. S. Cazzolato and Z. Prime, "On the dynamics of the Furuta pendulum," *Journal of Control Science and Engineering*, vol. 2011, p. 528341, Apr 2011.

[12] U. N. L. T. Alves, R. Breganon, L. E. Pivovar, J. P. L. S. de Almeida, G. V. Barbara, M. Mendonça, and R. H. C. Palácios, "Discrete-time $\mathcal{H}_\infty$ integral control via LMIs applied to a Furuta pendulum," *Journal of Control, Automation and Electrical Systems*, vol. 33, no. 3, pp. 1–12, 2022.

[13] H. Silva, I. Ramos, U. Alves, R. Cardim, M. Teixeira, and E. Assunção, "Switched control design with guaranteed cost for uncertain nonlinear systems subject to actuator saturation," *IFAC-PapersOnLine*, vol. 53, no. 2, pp. 8025–8030, 2020, 21st IFAC World Congress.

[14] U. N. L. T. Alves, "Robust switched control with guaranteed cost of a Furuta pendulum prototype using T-S fuzzy mode: Data," Mendeley Data, V3, 2026. [Online]. Available: https://data.mendeley.com/datasets/z2p4xw9hnd/3

[15] I. R. Petersen, "A stabilization algorithm for a class of uncertain linear systems," *Systems & Control Letters*, vol. 8, pp. 351–357, 1987.

[16] S. P. Boyd, L. El Ghaoui, E. Feron, and V. Balakrishnan, *Linear matrix inequalities in system and control theory*. SIAM, 1994, vol. 15.

[17] L. F. S. Buzachero, E. Assunção, M. C. M. Teixeira, and E. R. P. D. Silva, "New techniques for optimizing the norm of robust controllers of polytopic uncertain linear systems," in *Frontiers in Advanced Control Systems*, G. L. de Oliveira Serra, Ed. London: IntechOpen, 2012, ch. 4.

[18] J. Lofberg, "YALMIP: A toolbox for modeling and optimization in MATLAB," in *Computer Aided Control Systems Design, 2004 IEEE International Symposium on*. IEEE, 2005, pp. 284–289.

[19] P. Gahinet, A. Nemirovskii, A. J. Laub, and M. Chilali, "The LMI control toolbox," in *Decision and Control, 1994., Proceedings of the 33rd IEEE Conference on*, vol. 3. IEEE, 1994, pp. 2038–2041.